Deep Mining 2024 – P Andrieux & D Cumming-Potvin (eds)

doi:10.36487/ACG_repo/2465_89

Understanding rock mass–backfill interaction in support of deep and high-stress mining

Murray W Grabinsky [a,*], Ben Thompson [a], Mohammadamin Jafari [b], David B Counter [c], William F Bawden [d]

[a] *Paterson & Cooke, Canada*

[b] *University of Toronto, Canada*

[c] *Kidd Mine, Glencore, Canada*

[d] *Bawden Engineering, Canada*

Abstract

There is currently a need for better understanding of backfill design requirements at depth or under high-stress conditions, or in rock mass with poor quality. It is generally acknowledged that rock mass closure affects backfill performance but there is currently negligible practical guidance for a design engineer. Understanding how mining conditions induce closure onto backfill is essential, as is predicting the reaction of the backfill to passively supporting the rock mass. This paper introduces a new framework for backfill design incorporating closure conditions. Rock mass-backfill interaction is considered using parametric studies that consider the backfill's 'loading system' as a combination of field stress, rock mass stiffness and the evolving geometry associated with ongoing mining. Parameterisation is used so that the extent of potential rock mass closure can be estimated for different mining conditions. Then, stiffness contrasts between backfill and the rock mass are considered. Load transfer from rock mass to backfill must be understood, neglecting initial closure occurring before the open stope is backfilled. The resulting analysis framework predicts the extent to which backfill distress may be an issue and enables assessment of the efficiency of increasing backfill strength and stiffness for a particular design scenario. A critical determination is that opportunities to engineer the backfill's strength and stiffness to resist initial rock mass closure on the backfill when the adjacent stope is mined is limited to cases where stresses are relatively low and rock mass quality (evaluated using the geological strength index [GSI] or equivalent) is moderate to high. Conversely, in high-stress conditions the initial closure on the backfill may have negligible consequences if the rock mass quality is sufficiently high. These extremes are quantified for a particular mining method and geometry. However, the analysis approach is equally applicable to other mining methods and geometries, and the framework to tackle these different mining problems is provided.

Keywords: *rock mass closure, backfill, evaluating backfill efficiency in supporting rock mass*

1 Introduction

Many mines must define adequate backfill strengths to enable backfill undercutting or sidewall exposures. Numerical modelling approaches are recommended, but under 'typical' conditions, empirically defined analysis based on beam theory for undercutting or net weight analysis (i.e. arching) for sidewall exposure provide reasonably conservative design strengths (Grabinsky & Thompson 2024a, b). Under most circumstances this design process ignores rock mass interaction. For deep, high-stress or high closure mining conditions, however, rock mass interaction with backfill arguably requires careful consideration. Sainsbury & Urie (2007) included such consideration, concluding that 'due to the increase in (elastic) modulus and 'brittleness' with increasing (backfill) strength…(backfill) strength beyond 275 kPa (Unconfined Compressive

[*] Corresponding author. Email address: murray.grabinsky@patersoncooke.com

Strength, UCS) does not result in an increase in stability' for their considered narrow-span undercut scenario. Other designers have neglected the role of confinement on backfill provided by rock mass closure. In one case, a 6–10 MPa UCS backfill was proposed for a cut-and-fill stoping design where plausibly empirical methods would suggest 2 MPa was adequate (reference withheld). This paper therefore aims to provide a design framework based on a fundamental understanding of rock mechanics and backfill geomechanics. This is motivated by the growing need to optimise design practices, leading to the reduced consumption of cement in mining while maintaining a conservative design from a safe operational perspective.

The geotechnical engineering phrase 'soil-structure interaction' is conventionally used in the context of civil engineering problems including tie-back shoring walls, backfilled gravity retaining walls, buried culverts, laterally loaded pile foundations and raft foundations for relatively broad but shallow footing systems. In such problems the 'structure' is clearly distinct from the 'soil' and the structural system is stiffer than the soil. The essential concepts of soil-structure interaction can also be found in the new Austrian tunnelling method and similar methods for rock mass support of larger underground structures such as power caverns and mining stopes. Arguably the same approach should also be used to understand the interaction between mine backfill and the excavated rock mass. Examples can be found in the literature of attempts to model specific examples of backfill-rock mass interaction, but a generalised approach has yet to be suggested. Therefore the primary objective of the present work is to propose an approach to characterise backfill-rock mass interaction for mining problems, and to demonstrate this approach for a particular mining and backfilling sequence. The following section presents a hypothesis for the modelling approach and a literature review relevant to the subsequent modelling. Analysis results are then generalised and implications for understanding the 'rock mass loading system' on the backfill are considered. Case study observations are also provided, emphasising the need for calibration of analysis with field-based validation.

2 Background

2.1 Hypothesis

The essential hypothesis for this work is as follows:

1. The 'rock mass loading system' responsible for rock mass closure on the backfill can be characterised by (a) the ratio of the field stress to the rock mass stiffness (i.e. increasing field stress and/or decreasing rock mass stiffness leads to increasing closure potential on the backfill), (b) the excavation geometry, which evolves with ongoing mining, and, potentially, (c) structural geology.
2. The effectiveness of the interaction between the backfill and the rock mass can be characterised by the ratio of the backfill stiffness to rock mass stiffness (i.e. the lower this ratio is the less effective the backfill will be in controlling closure).

Note that the two ratios indicated above are generic and could be used for any mining scenario, and while the geometry is problem-dependent it can be idealised for some commonly used mining methods.

A restrictive assumption used in the present work is that the rock mass can be considered linear elastic. This is clearly not always the case but there are examples of very large open stopes in unsupported rock mass that remain open and stable for many months (e.g. the roughly 30 × 30 m plan dimensions by 130 m-high stope in Canadian Shield rock mass at about 0.5 km depth, as described by Mitchell et al. 1975). Even if the surrounding rock mass requires support to remain stable while the stope is open, the extent of damage must be less than the maximum stope dimension. But the more important driver for deformation is the total mining excavation and the rock mass must be predominantly elastic in this larger geometric context. Therefore rock mass damage proximate to the stope will be ignored.

Another restrictive assumption is that the backfill can be considered linear elastic. While this is an over-simplification in general, for large strains the elastic modulus used should be the secant modulus rather than the tangent modulus of the intact material. Future work may consider adapting the approach described in the present work to incorporate nonlinear backfill response when warranted.

2.2 Case studies

Laboratory testwork and field measurements were carried out for uncemented hydraulic fill in a thin tabular orebody at less than 0.5 km depth at a Boliden mining operation in Sweden (Knutsson 1980). The 1D stress–strain backfill response was measured in the laboratory using oedometer tests, and closure displacements during mining were used to calculate strains and therefore estimate the backfill reaction stress during closure. Backfill self-weight effects were calculated using arching theories based on 'silo theory' (i.e. Janssen 1895) but modified for stope inclination. The combination of self-weight effects and arching effects matched well with field measurements of closure stress in the backfill. Closure displacements and computed strains were not reported, but in general the research concluded that 'the stress component caused by the convergence is responsible for 20–30% of the total stress. This rather small contribution indicates that the influence of the backfill on the stress situation in the confining rock is practically negligible'. This case study demonstrates that the 'rock mass loading system' can be stiff enough to be ignored for backfill design in some cases.

An experimental approach like that described for Näesliden mine was used at Lucky Friday mine (Raffaldi et al. 2019). The cemented paste backfill (CPB) used at Lucky Friday is among the strongest and stiffest reported (Grabinsky et al. 2022). The orebody is essentially vertical with cut-and-fill stopes about 3 × 3 m in cross-section. Tight filling methods are not used. The studied stopes were at about 2 km depth and were monitored during five successive undercuts. The closures resulted in a roughly linear trend with undercut number, resulting in 8–5% closure strain. Peak stresses occurred after the first undercut, with declining stress thereafter suggesting the backfill was being strained into the post-peak regime. This case study demonstrates the opposite to the case above, i.e. there can be situations where the rock mass loading system is so dominant that the backfill stiffness is inconsequential to limiting rock mass convergence and therefore the backfill must be designed to accommodate large closure strains.

An early attempt to measure the CPB response to mining was reported by Hassani et al. (2001) at Chimo mine in Quebec, Canada. Three adjacent stopes (with the middle void mined last) were evaluated. Average stope thickness was 4.0 m and the maximum closure strain in the previously placed backfill was 8% after the last void was mined (i.e. 32 cm over the 4 m span). They also noted that a subsequent rockburst with a magnitude representative of regional mining-induced seismicity only increased backfill stresses and strains by some 10% compared to the pre-existing strain, suggesting that closures due to proximate mining dominates the induced backfill stresses and strains. They considered their results consistent with eight earlier field studies.

These case studies demonstrate the wide range of rock mass loading system responses that can be encountered in mining. Rock mass-backfill interaction must therefore be considered as follows: firstly, the initial closure of the rock mass on the most recently placed backfill occurring with the subsequent mining stage must result in strains suitably small that the backfill is not immediately crushed; and secondly, with ongoing mining the backfill will most likely be driven into the nonlinear interaction range, and the reaction this provides to global rock mass stability needs to be better understood. The subsequent analysis will attempt to characterise rock mass-backfill interaction to address these issues.

2.3 Backfill material properties

As just noted, the relevant backfill material properties for the analyses that will be presented are the stress–strain behaviour under low confining stress when the first closure occurs on the most recently placed backfill, and the confined compression response at later mining stages as ongoing mining continues to load the backfill under fully confined conditions. Grabinsky et al. (2022) considered a wide range of CPB (and other) materials tested by many organisations/mines and correlated the Young's modulus and UCS results, finding that the relation is approximately linear for a given material although the correlation constant varied by about an order of magnitude for all materials within the dataset. Therefore in the current work, the backfill stiffness (Efill) is correlated to the strength using Efill = 250 UCS, although sensitivity studies could consider values ranging from one-third to three times these values. Also, most samples reach peak strength (UCS) at about 1 to 2% axial strain. Jafari et al. (2021) conducted drained triaxial testing on the Williams mine CPB under relatively low confining stress conditions (confining stresses about 0.0446, 0.1786, 0.3571 and 0.6250 of UCS for the strongest material considered) and showed that strain to peak strength increases as the relative confining stress increases, up to 12% for the highest confinement used. Therefore in this work, 2% rock mass closure strain is considered a critical value in that it likely coincides with the onset of backfill failure under relatively unconfined conditions.

Jafari et al. (2020) tested CPB samples in 1D compression and interpreted the results as 'ground reaction curves', showing how backfill reaction to stope closure increases exponentially up to 15% strain. However, a linear approximation to these curves using the secant modulus at 2% strain generates values of secant modulus comparable to the tangent Young's modulus from UCS tests, and the maximum error in stiffness compared to the nonlinear reaction curve is about 25% at 9% axial strain. Given the parametric nature of the studies carried out here, this linear approximation is considered appropriate and so Efill will be used to represent the backfill stiffness over the full range of rock mass closure.

2.4 Rock mass material properties

As previously argued, the global rock mass system will be characterised as linear elastic. In lieu of a more detailed assessment of rock mass stiffness, the simplified Hoek & Diederichs (2006) relationship between Young's modulus and the geological strength index (GSI) is used (with damage parameter *D* set to zero).

$$E_{rm}(MPa) = 100{,}000\left(\frac{1-D/2}{1+e^{\left(\frac{75+25D-GSI}{11}\right)}}\right) \tag{1}$$

2.5 Previous modelling studies

2.5.1 Analytical models

The significance of rock mass closure on backfill response in the context of undercut backfill exposures, (also termed a 'sill mat') was originally recognised by Mitchell & Roettger (1989), who stated that 'If the expected rock movement is estimated, it is possible to engineer the cemented sill so that the lateral prestress is a considered design condition, giving σ_c = E δ/L. The order of magnitude of the sill stiffness modulus, E, may be controlled by the cement content used and it is suggested that σ_c should be less than 50% of the plain strain unconfined compressive strength of the cemented fill'. (Note that σ_c is the average compressive stress due to rock mass closure δ, and L is the undercut span.)

The irony of this 'considered design condition' is that a high-strength backfill should presumably be more capable of resisting rock mass closure, but a stronger backfill also has increased stiffness and therefore, for a given δ/L, attracts higher induced stress. Thus there must be some practical limits to the rock mass loading system as defined in the hypothesis (Section 2.1) under which the design backfill strength and stiffness is plausible. Such practical limits are certainly not obvious and have not been considered in detail in the literature. Perhaps this is why, in the later version of the analysis method published by Mitchell (1991), the crushing criterion was not considered.

2.5.2 Numerical models

Other authors have recently considered backfill-rock mass interaction for specific case studies, however, typically there is not appropriate consideration of the detailed material properties and correlations between the properties previously discussed. For example, Wang et al. (2021) correctly note that backfill's compressibility is equally as important as its shear strength, yet in their undercut backfill case study the sill mat is modelled with UCS of 20 MPa and Young's modulus 1.5 GPa. This UCS is significantly higher than typically used mine backfill (i.e. Grabinsky et al. 2022). A 20 MPa UCS backfill is like concrete, for which the Young's modulus is about 20 GPa. For the problem considered, if the rock mass loading system is stiff compared to the sill mat, then a 20 GPa stiffness material will attract an order of magnitude more stress than a 1.5 GPa stiffness material, which highlights the importance of choosing values for material parameters that are consistent with typical mine backfill materials. Similarly Keita et al. (2022) conducted a numerical analysis of sill mat stability where the critical cohesion is determined as a function of backfill stiffness, among other parameters. Not varying strength and stiffness in a consistent way contradicts the findings of many researchers, as discussed in Section 2.3.

Finally, in a reinterpretation of sill mat strength requirement estimates based on the method of Pakalnis et al. (2005), Grabinsky et al. (2022) note that many mines use strengths much higher than those indicated by the suggested design method. One of the reasons suggested for this is the high closure potential (as in the Lucky Friday case study) and the belief that higher strength backfill will provide better resistance to closure. Whether or not this could be possible is investigated in the context of a particular mining scenario in the next section.

3 Numerical experimental methodology

The numerical analysis considered here is for a particular mining scenario and associated geometry, although the approach can be applied to any mining method and geometry. A series of stopes 2 × 2 m in vertical cross-section and very long are considered such that the analysis can be conducted as 2D plane strain. Fifteen stopes in total are modelled in a sequential mining/backfilling progression. In addition to the specific geometry, the rock mass loading system is normalised with respect to a unit isotropic field stress of 1 MPa and a unit rock mass stiffness of 1 GPa. Because the system is linear elastic the analysed displacements can be multiplied by the actual isotropic field stress (in MPa)/actual rock mass stiffness (in GPa) for other rock mass conditions. Different analyses are carried out using backfill stiffness to rock mass stiffness contrasts of 0, 10, 25, 50, 100 and 150%. The displacements are then analysed to assess the effectiveness of the backfill in controlling rock mass displacements. Analyses were carried out using the finite element program RS2 from Rocscience Inc. Additional modelling details will be provided subsequently.

3.1 Geometry and mesh

If gravitational forces are ignored (i.e. the initial field stress dominates the stress distribution) the modelled problem is symmetric about a horizontal axis running through the stopes' mid-heights (Figure 1). As such, the same result would be obtained if the model was rotated 90° to simulate mining a vertical tabular orebody. The length of the simulated horizontal tabular orebody (i.e. reef) is 30 m. The outer limits are extended to 30 m from either end of the reef, and vertically to 45 m above the reef centreline. The boundary conditions on the vertical extents are rollers allowing only vertical displacements. The boundary condition on the lower symmetry line are rollers allowing only horizontal displacement. The top horizontal boundary is loaded with a 1 MPa pressure to match the initial field stress. A sensitivity study was not carried out on this geometry or boundary conditions, however, the approach follows generally accepted good modelling practice in the primary author's opinion.

Finite elements are six-noded triangles, graded to provide maximum concentration in and around the modelled stopes. A mesh refinement study was carried out. Mesh density shown in Figure 1 was deemed adequate for current purposes. There are approximately five elements through the modelled stope's half-height, and about 3,800 elements in total. All elements passed RS2's built-in mesh quality check function.

3.2 Field stress

There are two useful idealisations with analytic solutions to assess the influence of the field-stress condition and the excavation geometry on the resulting stress and displacement distributions: (1) the Kirsch solution for a circular hole, and (2) the Griffith solution for an infinitesimally thin crack. Whereas the Kirsch solution is sensitive to field stresses in both principal directions, the closure of a Griffith crack is only sensitive to a principal stress normal to its surface. The modelled geometry is closer to a Griffith crack than it is to a circular hole, therefore it can be assumed that the field stress normal to the modelled reef is primarily responsible for the analysed closure displacements. However, the closure displacement's sensitivity to the horizontal field stress could be explored with further modelling, if deemed necessary. The magnitude of the field stress can be estimated in the vertical direction based on assumed overburden (i.e. about 27 MPa/km depth), which is useful for a reef model, but for vertical tabular orebodies, estimating the horizontal stress is more variable (see the guidelines in Hoek 2023).

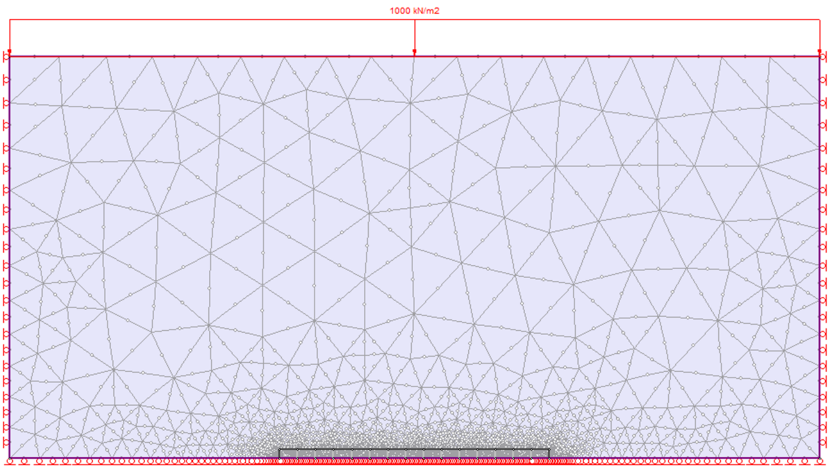

(a)

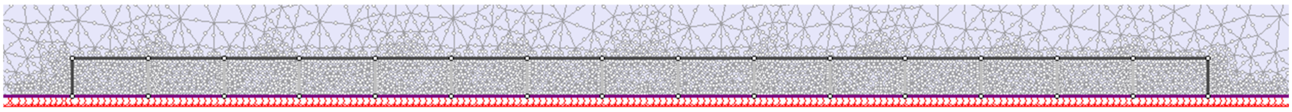

(b)

Figure 1 Model geometry and finite element mesh used for numerical analysis: (a) Entire model; (b) Close-up view of 15 stopes modelled for excavation and backfilling. Note that the lower bound of the model is a line of symmetry

3.3 Rock mass stiffness (Young's modulus)

As discussed in Section 2.4, the equation for estimating rock mass Young's modulus based on GSI only is appropriate for this parametric study due to its simplicity. However, a more refined estimate of rock mass Young's modulus (and especially the intact rock modulus) is appropriate where data exists.

3.4 Backfill stiffness to rock mass stiffness contrast

Using the intact material backfill stiffness ranges from Grabinsky et al. (2022), an equivalent range of rock mass stiffness based on GSI can be determined using Equation 1, as shown in Table 1. Note that as the rock mass GSI increases beyond 40, even the strongest and stiffest backfills available will have intact backfill Young's modulus (Efill) compared to rock mass Young's modulus (Erm) ratios (i.e. Efill/Erm) diminishing from 1.0. In the analysis results presented, the Efill/Erm contrasts of 10, 25, 50, 100 and 150% will be used.

Table 1 Estimates of upper-bound and lower-bound equivalent rock mass geological strength index to match the backfill stiffness for given backfill unconfined compressive strength

UCS (MPa)	0.5	1.0	2.0	3.0	4.0	5.0
GSI min	0	0	6	13	18	20
GSI max	10	22	30	35	37	40

4 Numerical analysis results

4.1 Total closure results

Due to the geometry used (i.e. 2 × 2 m stopes) the vertical displacement of each stope's top surface is the same as the closure strain (e.g. a closure of 3 mm over the 1 m stope half-height is a closure strain 0.003 or 0.3%). The midpoint of each stope's top surface is used as the monitoring point for representative stope closure. It is useful to compare the effectiveness of the Efill/Erm contrast on limiting the maximum global closure once the stopes are completely mined and backfilled. This is shown in Figure 2. Recall that the closure strain is proportional to the field stress (in MPa)/rock mass stiffness (in GPa) ratio for an actual mining problem, and for the closure strain results shown the ratio used is 1. However, on a comparative basis, there is a limit to the backfill's efficiency in the sense that peak global closure strains (e.g. 0.0122 for Efill/Erm = 50% as shown in Figure 2) are dramatically reduced as the Efill/Erm contrast increases from 0 to 50%, but then increasing Efill/Erm from 50 to 100%, and then again from 100 to 150%, becomes incrementally less effective. Therefore designing backfill to be stiffer than the surrounding rock mass appears inefficient. Note that even an infinitely stiff backfill cannot completely prevent closure. This is because, after excavation, there will be some closure before the backfill is placed.

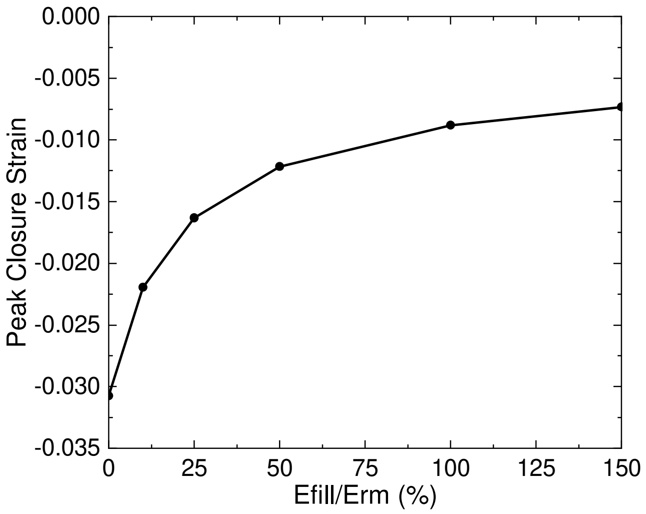

Figure 2 Maximum global closure strain after excavating and backfilling, for different Efill/Erm contrasts

4.2 Incremental closure results

From the perspective of the individual stope the critical closure occurs immediately after the stope is backfilled and the adjacent stope excavated. The reason this is critical is that, for tight filled stopes, this is the only time when the backfill will experience closure under conditions of one exposed face; thereafter the backfill will undergo closure in confined conditions. One way to understand this critical closure condition is to examine the closure increment occurring on the backfill immediately after placement and after excavation of the next stope. This data is obtained from the primary global closure data. The trends for each incremental stope excavated, and for various Efill/Erm contrasts, is presented in Figure 3. Examining the slope of each trend line in Figure 3, after the fourteenth excavation the backfills undergo essentially linearly increasing rates of convergence, and these rates are quantified in Figure 4. The interpretation of this trend is like that for global peak closure strain (Figure 2) except that the trend is even more extreme. The combined interpretations challenge the notion that an extremely stiff backfill (i.e. Efill/Erm > 1) can effectively prevent rock mass closure; rather, there is some efficiency to be realised for Efill/Erm up to perhaps 50%, beyond which the rock mass system stiffness will dictate the closure strains.

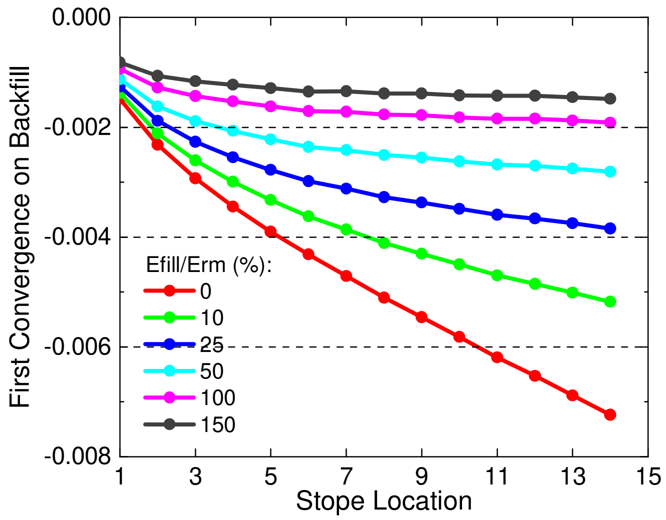

Figure 3 First closure strain on freshly placed backfill after adjacent stope excavation, for each stope in the sequence and for various Efill/Erm contrasts

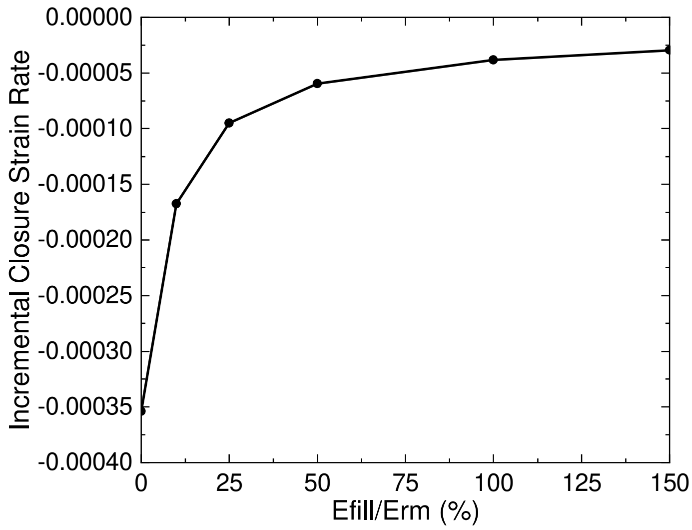

Figure 4 Incremental closure strain rate after excavating the fourteenth stope, for various Efill/Erm contrasts

4.3 Field-stress/Erm scale factors required to cause backfill failure

Although the incrementally placed backfill considered in the previous section has one exposed face, the stress distribution within the backfilled stope is far from 1D. Considering the backfill triaxial test results presented in Jafari et al. (2021), the average strain to failure is more likely to be in the range of 4 to 8% (corresponding to confining stress/UCS = 0.0446, 0.1786). In this case the scale factor (field stress/Erm) can be determined from the incremental closure results that would produce the specified strains. This is shown in Figure 5 (note that the vertical scale is logarithmic). These scale factors are directly proportional to the convergence value chosen. The figures could be useful to determine, for mining geometries like that used for the analysis, what the scale factors would be for a given Efill/Erm contrast and for a given number of excavations that could cause distress in the backfill upon first closure with mining of the adjacent stope.

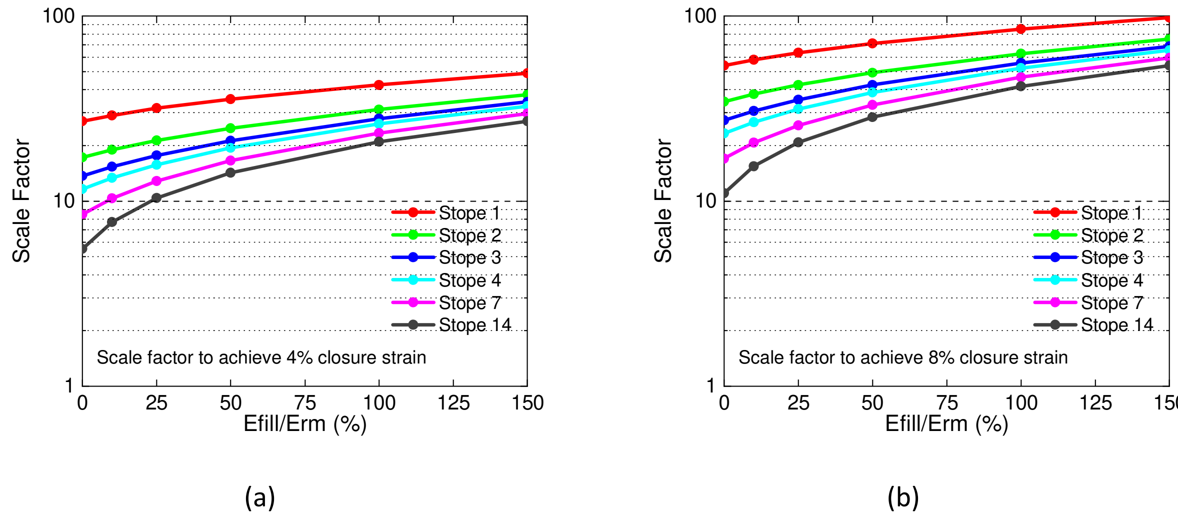

Figure 5 **Scale factors (field stress/Erm) required to achieve (a) 4% and (b) 8% initial closure strain on backfill**

4.4 Field-stress/Erm scale factors required to prevent backfill failure

Like the above analysis, the other extreme would be to determine the scale factors required to prevent backfill failure upon first closure with mining of the adjacent stope. For the purposes of the present parametric study, based on the failure strain for different CPB UCS tests and also as can be observed for a low confined triaxial test (Jafari et al. 2021), a critical value of 2% closure strain is chosen as a conservative heuristic. For a given GSI and computing Erm using Equation 1, the lower-bound stress level required to achieve 2% closure strain occurs using the Efill/Erm = 0 curves. The upper bound stress level required to achieve 2% closure strain occurs using the Efill/Erm = 100% curves. The results are presented in Figure 6, and demonstrate that the range over which backfill can be 'practically engineered' to control rock mass displacements is very limited compared to the broad range of possible mining conditions (i.e. stress and rock mass stiffness). The detailed mining conditions shown in Figure 6b for depths 1 to 5 km and GSI 40 to 75 indicate that conventional backfills will have low Efill/Erm contrasts and therefore the opportunity to practically engineer these fills to control rock mass closure displacements is limited.

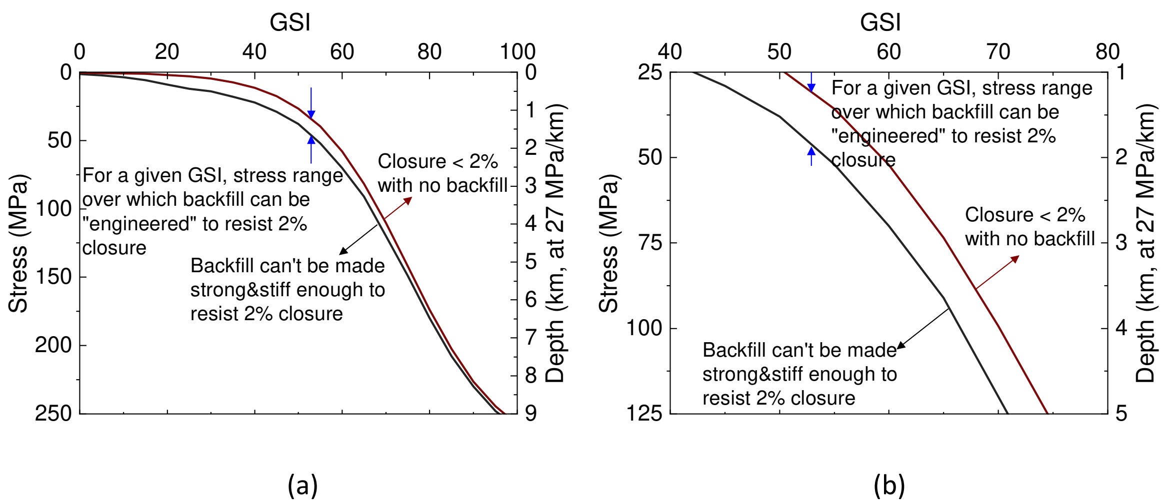

Figure 6 **The range of rock mass conditions over which backfill can be practically engineered to resist rock mass closure upon first exposure after mining of the adjacent stope: (a) Global mining conditions; (b) Detailed mining conditions**

5 Example design scenarios

The approach described in the previous section was incorporated into a design spreadsheet tool to help visualise specific mining conditions, an example of which is shown in Figure 7. The essential input is field stress (either entered directly or as a function of depth below surface), rock mass stiffness (either entered directly or as a function of GSI) and backfill Young's modulus as a factor of UCS. In the provided example the field stress is 25 MPa, the rock mass GSI is 25 and Efill = 250 UCS. Backfill effectiveness in controlling rock mass convergence is plotted for the last backfilled stope in the modelled mining sequence. The displayed design curve indicates that a mining sequence with backfill strength UCS = 500 kPa or less will generate closure displacements in the range 12 to 18%, but even a very strong (5 MPa UCS) backfill cannot limit the closure displacements to less than 4%. This result is consistent with where the rock mass conditions plot on Figure 6.

Input:						Notes:
Field Stress	Enter the field stress value....	25	MPa			
	OR enter **zero** above and enter a depth....			0	km	Stress is computed using 27 MPa/km
Rockmass	Enter the rockmass stiffness....	0	GPa			
	OR enter zero above and enter GSI....			25		Rockmass stiffness Erm is computed using the Hoek & Diederichs formula
Backfill	Enter the backfill Efill/UCS ratio	250				The average is 250; maximum value should be 500 and minimum 125

From the above input, use the following parameter values:

Stress	25	MPa
Erm	1.0503845	GPa
Efill/UCS	250	
Factor	23.800809	to multiply convergence for actual stress and Erm conditions

1st convergence on backfill placed in 14th stope

Efill/Erm (%)	scaled closure	Efill/Erm (%)	closure (%)
0	-0.00724	0	-17.231786
10	-0.005182	10	-12.332389
25	-0.003845	25	-9.1521252
50	-0.002812	50	-6.6927876
100	-0.001914	100	-4.5564269
150	-0.001481	150	-3.5241858

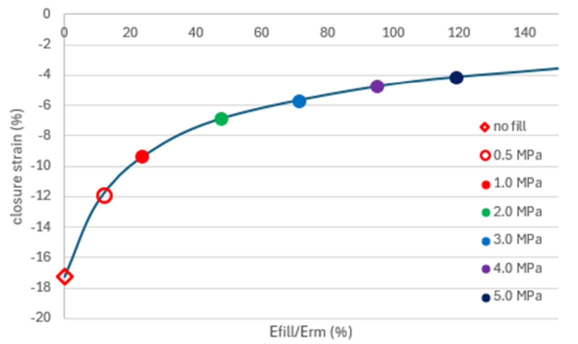

Figure 7 Example design calculation for 25 MPa field stress, geological strength index 25 rock mass and Efill = 250 UCS for the last backfilled stope in the reef model

A contrasting example is shown in Figure 8a, where the field stress has changed from 25 to 5 MPa. Now the displayed design curve shows that rock mass closure strains can be effectively limited to 2% using a 1 MPa UCS backfill. However, such a low field stress approximates only relatively shallow mining conditions. A final example is shown in Figure 8b for field stress 60 MPa and rock mass GSI 60. In this case the backfill can theoretically be engineered to limit rock mass closure to 2%, but from a practical perspective the difference in closure between the case of no backfilling and backfilling with the strongest available material is inconsequential. This is due to the rock mass being stiff relative to practically available backfill materials.

To summarise the implications of this analysis, Figure 9 compares the analysis framework defined in Figure 6 with data from Hughes' (2014) meta-study of several cut-and-fill operations. Note that these mines had horizontal stresses higher than the vertical stresses, and stress perpendicular to the orebody were assumed in the figure. The Stillwater and Lucky Friday mines undergo significant closure consistent with the proposed analysis method. Red Lake and Macassa do not have closure issues per se, but the high-stress and stiff rock mass conditions have presented significant rockburst management issues. Kencana is an outlier in the case histories because it is very shallow (a few hundred metres below surface) but only the lowest rock mass quality regions (GSI ~ 30) present any significant ground control issues. As mentioned in the Introduction, Sainsbury & Urie (2007) consider backfill strength requirements in a narrow vein orebody at Raleigh mine. The modelled rock mass stiffness was 50 GPa, which is consistent with GSI = 75 using Equation 1. The field stress magnitude is not mentioned but the combination of rock mass stiffness and field-stress-generated closure strains were deemed to be representative of field conditions. These conditions would be like those assumed in Figure 6b. Their conclusion that increasing backfill UCS beyond the recommended value had no beneficial effect is consistent with the trend suggested by Figure 6b.

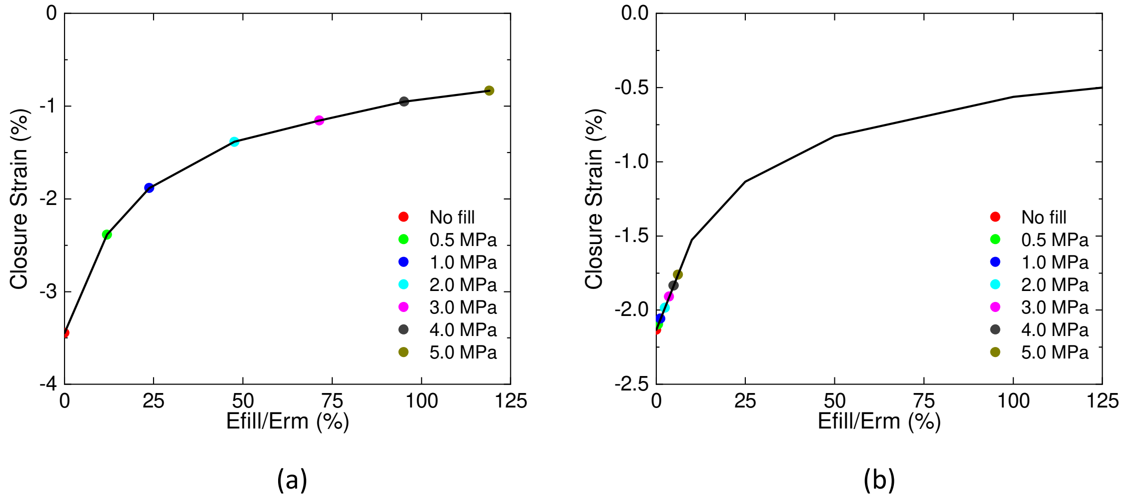

Figure 8 (a) Example design calculation for 5 MPa field stress, GSI 25 rock mass, and Efill = 250 UCS, for the last backfilled stope in the analysed model; (b) Example design calculation for 60 MPa field stress, GSI 60 rock mass, and Efill = 250 UCS, for the last backfilled stope in the analysed model

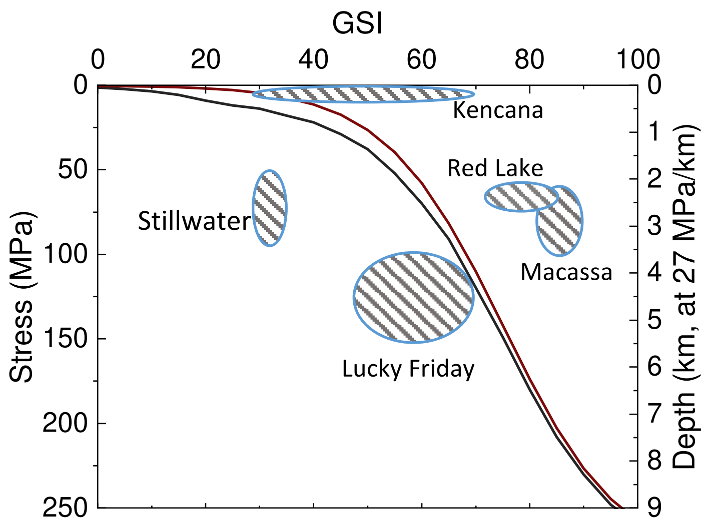

Figure 9 Comparison of underhand cut-and-fill mining operations from Hughes (2014) with the analysis approach developed in this work

6 Field observations and next steps

This paper presents a theoretical framework for consideration, and future work will involve further analysis of larger stopes and stope sequencing to assess design implications for larger backfill exposures. As ever, calibration of modelling with field observations is a critical component of rational design. Evaluation of practical outcomes as to how mines design backfill properties to account for, or mitigate against the effects of, closure will provide additional guidance for designers and represents a key next step in this design topic.

An excellent example of best practice backfill design is provided by Glencore's Kidd Mine (Ontario, Canada) which is one of the deepest base metal mines in the world. Evidence of how the rock mass response to mining influences fill behaviour is apparent as the mine's increasing depth has exposed the backfill to higher stress conditions. Measurements of pressures within backfilled stopes were earlier reported at Kidd (i.e. Thompson et al. 2009) as exceeding 1.3 MPa, at which point the instrument range was exceeded. Subsequent similar instrumentation work conducted at the mine indicates pressures within the backfill reached 3.5 MPa (which exceeds the unfactored UCS target), at which point they appeared to plateau. Field stresses are approximately 100 MPa.

Kidd's backfill design features numerical modelling (conducted by third parties) incorporating rock mass conditions, and regional and local stress states, to design strength requirements for relatively wide-span undercut backfill exposures. Modelling included steady-state closure. Backfill strength input properties for the modelling were determined from triaxial testing. For undercut spans of up to 20 m, fill strengths of 3.6 MPa UCS were required, which assumed a strength factor of 1.5. The mine poured plugs of 7 and 20 m height (sequence dependent) within the 40 m-high stopes.

Critically, sidewall backfill failures and some undercut exposure failures in high-stress abutments and tertiary mining areas have been observed at Kidd. The causes of backfill failures are varied, with a common trend that understanding the stress paths that backfill experiences aids the interpretation of failure mechanics. In one case for instance, fault slip-induced shearing of paste planes equivalent to the strike and dip of the fault resulted in slabs of paste from the backfilled sidewall peeling into the open stope on exposure. While such an event is beyond the scope of rational design (to predict or mitigate), such observations of backfill response are not, to our knowledge, documented in literature.

In another recently documented case at Kidd, an undercut CPB exposure caved upwards by 10–15 m. A portion of the backfilled stope had previously been undercut but tight filling was not then achieved, such that the backfill remained in a partially unconfined state (as local stress fields evolved). When the initially filled stope was subsequently exposed by secondary panel mining, and the resulting cave surface was examined, drone camera footage showed failure surfaces consistent with tensile failure as the confining stress was unloaded during the backfill exposure mining process. These observations were consistent with the stress model expectations for such areas where high degrees of closure were expected. Figure 10 shows examples from this failure in terms of conchoidal fractures, a probe drillhole into the paste showing the fracture plane from a different orientation and, finally, fractured slabs or blocks of CPB. This pervasive structure is consistent with tension cracks forming during unloading of the CPB as neighbouring stopes were mined. These observations illustrate the need for mines to account for, and potentially accommodate, the occurrence of backfill failure under high-stress/closure conditions.

Clearly the Kidd field example presents a significantly more complicated scenario than the simplified modelling analysis that has been the focus of this paper. The analysis of the idealised reef stopes indicates the limitations of backfill in influencing rock mass closure, and the challenges practitioners face when engineering backfill properties for deep or high-stress and closure conditions. The Kidd practical example indicates further that as operational conditions evolve, understanding stress conditions within the orebody and the potentially complex 3D geometrical sequencing defining the stress path the backfill undergoes can significantly aid interpretation of the backfill response. While the failures are relatively isolated events with, in this case, limited operational consequences aside from excess CPB dilution within a handful of stopes, they clearly show that the rock mass system cannot be neglected if a realistic prediction of backfill response is a design requirement. We are not aware of mines that have changed mining methods in response to failure of backfill due to deep/high-stress mining conditions, and so it may be that the extreme consequences of rock mass closure are consistent with occasional incidents of greater-than-expected dilution. Work to expand the practical database, both in terms of backfill design approaches and the consequence of high-stress/closure conditions upon backfill, will continue. Within the context of this paper the Kidd case study is well summarised by the site's analogy that the backfill response is like 'squeezing a marshmallow in a vice'.

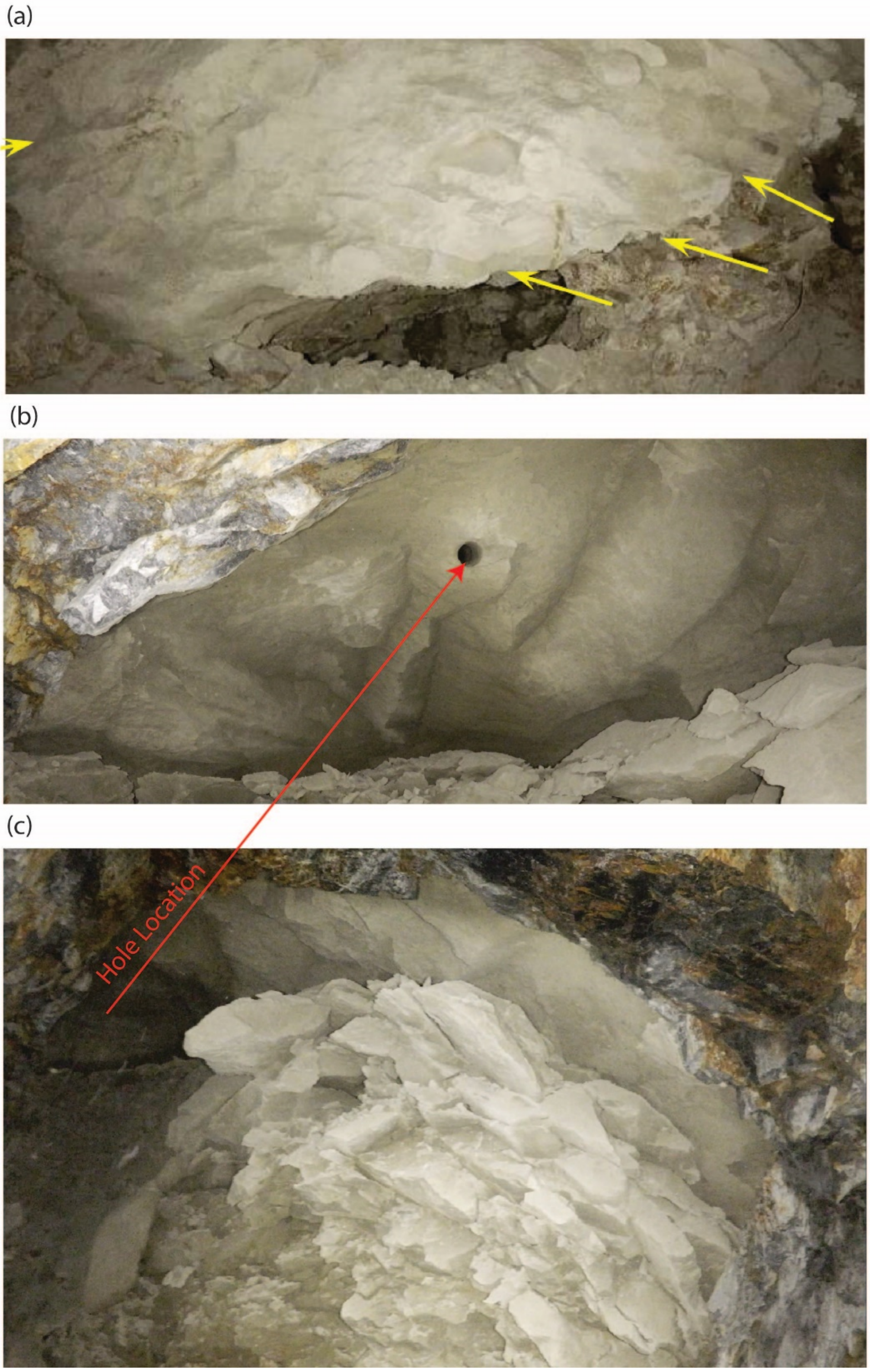

Figure 10 Images from Kidd mine showing structures in cemented paste backfill exposures: (a) Conchoidal fractures in paste above a void; (b) Strongly jointed paste due to induced stress and/or unloading of stress; (c) Interpreted tensile failures consistent with mining of the adjacent void

7 Conclusion

A rational model has been proposed to assess rock mass-backfill interaction in support of deep and high-stress mining. The rock mass loading system is characterised in terms of rock mass stiffness and field stress but also, very importantly, the evolving excavation geometry concurrent with ongoing mining. The interaction between stope closure and backfill reaction is characterised using Young's modulus of the backfill relative to the rock mass's modulus, Efill/Erm.

The most significant conclusions arising from the analysis are as follows:

1. A trendline is found for which combinations of rock mass stiffness and field stress greater than the trendline will result in insignificant initial closure on the backfill, in which case the backfill need not be intentionally engineered to resist such initial closure.
2. Conversely, a trendline is found for which combinations of rock mass stiffness and field stress less than the trendline will result in initial closure on the backfill so significant that the backfill strength and stiffness cannot possibly be engineered to prevent failure upon excavation of the adjacent stope.
3. Between the above extremes it is theoretically possible to engineer the backfill strength and stiffness to inhibit the initial closure on the backfill to a prescribed limiting strain of a few percent to prevent backfill failure upon excavation of the adjacent stope. However, the practicality of this engineered approach is limited to relatively shallow excavations, not characteristic of deep and high-stress mining.
4. Assuming mining strategies can be developed to prevent backfill failure upon excavation of the subsequent stope, the backfill's resistance to further rock mass closure with ongoing mining will inevitably drive the backfill into its nonlinear stress–strain response range. Therefore numerical models that attempt to model such response in support of rational mine design must incorporate backfill constitutive models capable of representing the backfill's nonlinearity.

With respect to the last point, to date there has been very limited relevant backfill testing to provide data to substantiate the required nonlinear models. Therefore more research is needed to generate the required data and to calibrate appropriate constitutive models.

Although the analysis presented here is specific to sub-horizontal or sub-vertical tabular orebodies, the outlined analysis method is general and can be applied to any mining method and associated geometry.

Acknowledgement

The authors wish to thank colleagues for informative discussions, particularly in terms of framing the cut-and-fill case examples. Modelling referenced in the Kidd case example was performed by Richard Brummer, Itasca Canada Inc. and Beck Engineering.

References

Grabinsky, M, Jafari, M & Pan, A 2022, 'Cemented paste backfill (CPB) material properties for undercut analysis', *Mining*, vol. 2, pp. 103–122.

Grabinsky, M & Thompson, BD 2024a, 'Progressive failure of undercut backfilled stopes: the problem with Mitchell's sill mat analysis', *Proceedings of* the *14th International Symposium on Mining with Backfill*.

Grabinsky, M & Thompson, BD 2024b, 'Elastic arching effects in tall cemented paste backfilled stopes', *Proceedings of* t*he 14th International Symposium on Mining with Backfill*.

Hassani, F, Ouellet, J & Servant, S 2001, 'In situ measurements in a paste backfill: backfill and rock mass response in the context of rockburst', *The 17th International Mining Congress and Exhibition of Turkey - IMCET2001*, pp. 165–175.

Hoek, E 2023, 'Chapter 6: in situ and induced stresses', *Practical Rock Engineering,* https://www.rocscience.com/learning/hoeks-corner

Hoek, E & Diederichs, MS 2006, 'Empirical estimation of rock mass modulus', *International Journal of Rock Mechanics and Mining Sciences*, vol. 43, pp. 203–215, http://dx.doi.org/10.1016/j.ijrmms.2005.06.005

Hughes, P 2014, *Design Guidelines: Underhand Cut and Fill Cemented Paste Backfill Sill Beams*, PhD Thesis, The University of British Columbia, Vancouver.

Jafari, M, Shahsavari, M & Grabinsky, M 2020, 'Cemented paste backfill 1-D consolidation results interpreted in the context of ground reaction curves', *Rock Mechanics and Rock Engineering*, vol. 53, pp. 4299–4308.

Jafari, M, Shahsavari, M & Grabinsky, M 2021, 'Drained triaxial compressive shear response of cemented paste backfill (CPB)', *Rock Mechanics and Rock Engineering*, vol. 54, pp. 3309–3325.

Janssen, HA 1895, 'Versuche über getreidedruck', *Silozellen Zeitschr*, vol. 39, pp. 1045–1049.

Keita, AMT, Jahanbakhshzadeh, A & Li, L 2022, 'Numerical analysis of the failure mechanisms of sill mats made of cemented backfill', *International Journal of Geotechnical Engineering*, vol. 16, no. 7, pp. 802–814.

Knutsson, S 1980, *Näesliden Project: Stress in the Hydraulic Backfill From Analytical Calculations and in situ Measurements*, internal report, Division of Soil Mechanics, University of Luleå, Luleå, https://www.osti.gov/etdeweb/servlets/purl/8489209

Mitchell, RJ 1991, 'Sill mat evaluation using centrifuge models', *Mining Science and Technology*, vol. 13, pp. 301–313.

Mitchell, RJ & Roettger, JJ 1989, 'Analysis and modelling of sill pillars', *Innovations in mining backfill technology*, CRC Press, Boca Raton, pp. 53–61.

Mitchell, RJ, Smith, JD & Libby, DJ 1975, 'Bulkhead pressures due to cemented hydraulic mine backfills', *Canadian Geotechnical Journal*, vol. 12, pp. 362–371.

Pakalnis, R, Caceres, C, Clapp, K, Morin, M, Brady, T, Williams, T, Blake, W & MacLaughlin, M 2005, 'Design spans-underhand cut and fill mining', *Proceedings of the 107th CIM-AGM*, pp. 1–9.

Raffaldi, MJ, Seymour, JB, Richardson, J, Zahl, E & Board, M 2019, 'Cemented paste backfill geomechanics at a narrow-vein underhand cut-and-fill mine', *Rock Mechanics and Rock Engineering*, vol. 52, pp. 4925–4940.

Sainsbury, DP & Urie, R 2007, 'Stability analysis of horizontal and vertical paste fill exposures at the Raleigh mine', *Minefill 2007 – Innovation and Experience: Proceedings of the 9th International Symposium on Mining with Backfill*, paper no. 2527, Canadian Institute of Mining, Metallurgy and Petroleum, Montreal.

Thompson, BD, Counter, DB, Grabinsky, MW & Bawden, WF 2009, 'In-situ measurements of cemented paste backfill in long-hole stopes', in M Diederichs & G Grasselli (eds), *ROCKENG09: Proceedings of the 3rd CANUS Rock Mechanics Symposium*.

Wang, R, Zeng, F & Li, L 2021, 'Applicability of constitutive models to describing the compressibility of mining backfill: a comparative study', *Process*, vol. 9, no. 2139, pp. 1–30.